

## Design and Analysis of All Optical Switch Based on Photonic Crystal Microcavity

Hamed Alipour-Banaei

Electrical Department, Faculty of Engineering  
Tabriz Branch, Islamic Azad University  
Tabriz, Iran  
h\_alipour@tabrizu.ac.ir

Afsaneh Asghariyan Tabrizi

Electrical Department, Faculty of Engineering  
Tabriz Branch, Islamic Azad University  
Tabriz, Iran  
asghariean@yahoo.com

**Abstract**— In this paper demonstration of all optical switch based on photonic crystal microcavity resonator has been done. The structure is based upon a nanowire photonic crystal geometry and consists of a patterned high refractive index thin film, supported by a  $\text{SiO}_2$  substrate. The proposed Switch has introduced a very narrow bandwidth and its quality factor is calculated by 160,000 compared with other samples has a significant increase and a footprint of only  $5\mu\text{m}^2$ . Simulation results are interpreted by means of FDTD simulations.

**Keywords**- Photonic crystal; microcavities; waveguides

### I. INTRODUCTION

Ultra small micro cavities that durably trap photons in small volumes close to the diffraction limit are essential components for modern optics and various related fields [1]. Although it is true that the physical phenomena observed in those cavities are similar to those previously reported in more conventional resonator etalons, micro cavities allow the performance to be boosted by orders of magnitude and offer a reliable platform for dense integration. They are characterized by two main quantities: the mode volume  $V$  and the quality factor  $Q$ . The former represents the spatial extent of the electromagnetic confinement and the latter is proportional to the photon lifetime in the cavity. Thus  $Q$  and  $1/V$  can be seen as the spectral and spatial energy density associated to the resonant mode, respectively. When trapped for sufficiently long times in a small space, photons strongly interact with the host material and thus create significant nonlinear [2], quantum [3] and optomechanical [4] effects, to quote only a few of them. The modification of the spontaneous emission rate of atoms placed in resonance with the microcavity mode is an emblematic effect. The combination of one-dimensional photonic crystal (PhC) structures with narrow waveguides in high refractive index contrast materials, such as silicon-on insulator, can satisfy all the requirements. Switching devices are essential components for processing of the signal when designing an all-optical integrated circuit (IC). Although a few proposals have been demonstrated based on non-optical modulation mechanisms, such as thermo-optic [3–5] or electro-optic [6–10] control, it is widely acknowledged that all-optical switching is the most promising technology towards. Unfortunately, the optical nonlinearities commonly used to modulate the signal are weak in Silicon, thus requiring large interaction lengths, as in devices like Mach-Zehnder [11]

interferometers or sizeable operational powers. As it has been shown in a number of papers [12–14] the problem can be solved by using optical resonators, which are able to enhance light matter interaction the achievement of faster response times in signal processing. This strengthened interaction makes it possible to exploit weak optical pump pulses to induce a significant resonance shift for a probe beam, thus achieving all-optical switching operation. For this purpose, PhC cavities are very promising, thanks to their high quality factors ( $Q$ ) and small modal volumes ( $V$ ), which allow for strong light-matter interaction on sub wavelength length scales. On one hand, the maximum light intensity inside the cavity is proportional to the ratio  $1/V$ , on the other, the required wavelength shift to obtain full switching is proportional to  $1/Q$ . The overall effect is a reduction of the power required to switch the signal by a factor  $Q/V$ , which can be very large in a PhC nanocavity. The switching power can be even proportional to  $Q/V$  if both probe and pump beams are resonant with the cavity modes. It thus becomes feasible to achieve an all-optical switching component working with a low enough control power to be integrated on a chip. The physical volume of the cavity has an important effect on the device commutation speed as well, because the relaxation time depends on the size when dealing with carrier-induced refractive index variations [16]. Furthermore, it is very important to achieve such interaction strengths in a system that presents the highest possible transmission, together with reduced losses, which is required for efficient processing of the signal. As compared to earlier pioneering work on this subject, a device having all these characteristics at the same time is still being developed. Recently, high- $Q$  PhC nanocavities in photonic wire (PhW) waveguides made of silicon-on-insulator wafers were successfully demonstrated [17–19]. Photonic wire waveguide mirrors, that consist of a periodic array of holes realized in a silicon wire on a silicon dioxide cladding layer, have very low propagation losses in a mechanically more robust system as compared to air-bridge structures. Nanocavities in photonic wires yield very high quality factors with low modal volumes, therefore, good candidates for applications as integrated photonic devices with small footprint, high mechanical stability, and strong enhancement of radiation-matter interaction. In this work, In this paper, we report a 1D cavity in a thin silicon layer with  $(\text{SiO}_2)$  under cladding, namely a silicon-on-insulator structure (SOI).

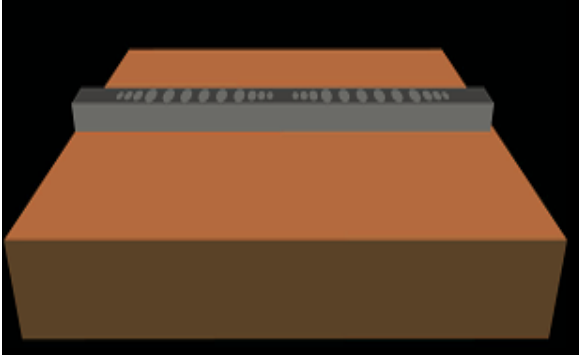


Figure 1. Sketch of the tapered PhC cavity embedded in a PhW waveguide with two mirrors composed by periodically spaced holes and aperiodic taper region inside and outside the cavity. The cavity in SEM picture has 6 holes in each mirror spaced by 350 nm and identical aperiodic taper region inside and outside. The spacings between adjacent holes are 300, 315, and 325 nm respectively. The corresponding hole radii are 65, 80, 85 nm.

High-Q, small-V linear Fabry-Perot micro-cavities manufactured in ridge waveguides on silicon-on-insulator wafers without removing the silica cladding. First, we briefly describe the characterization set-up, we detail the optical properties of the microcavities in terms of Q factor, transmittance and losses. Finally, we discuss the increase of cavities performances with the help of a predictive model.

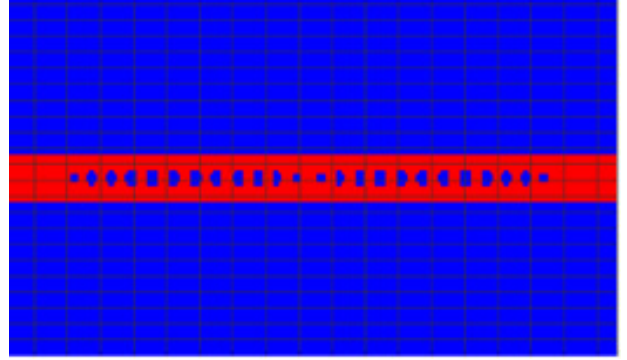
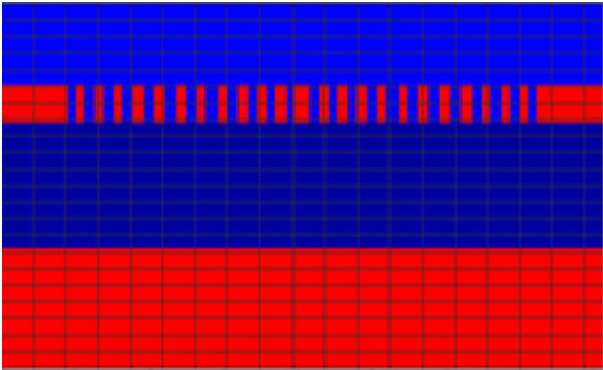
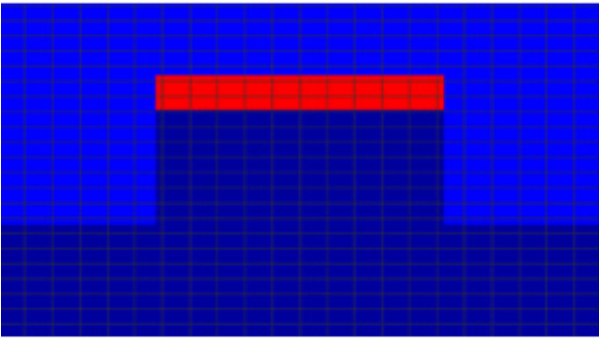


Figure 2. Sketch of the SILICON-ON-INSULATOR WAFERS wafers with a 260 nm silicon core layer supported by a 1  $\mu\text{m}$  silica layer. a: X-Y b: Y-Z c: X-Z

## II. SAMPLE DESCRIPTION

The samples employed in the present work were fabricated on SILICON-ON-INSULATOR wafers having a 0.26  $\mu\text{m}$  silicon core layer supported by a 1000 nm silica layer. The device is realized within a 1D PhC/PhW nanocavity structure consisting of a single row of circular holes embedded in a 0.5  $\mu\text{m}$  wide PhW waveguide with a lattice constant  $a = 0.35 \mu\text{m}$  and  $r/a = 0.28$ . The photonic crystal mirror is designed to exhibit a large stop band for TE polarization. To reduce the out-of-plane scattering, i.e. to increase simultaneously the cavity mode Q-factor and the absolute transmittance of the system, the mismatch between the waveguide modal effective index ( $n_{wg} = 2.9$ ) and the Bloch mode index ( $nB = 2.07$ ) is adiabatically reduced through proper cavity design. The regions within the cavity and between the mirrors and the waveguide are carefully tapered by means of holes with different diameters and significantly aperiodic spacings [22, 23], which makes it possible to reduce and recycle the mirror losses due to out-of-plane scattering induced by optical impedance mismatch. Different cavity lengths with different mirror hole numbers and taper geometries have been realized in order to enhance the Q factor. A sketch of the cavity with the two mirrors and tapers is presented in Fig. 1. The figure shows a 0.5  $\mu\text{m}$  wide photonic wire nanocavity formed by two mirrors, each of which includes a periodic array of six holes with the same diameter. Gradually tapered hole arrangements with different spacing and diameters are used inside and outside the cavity (three holes in each taper region, yielding a total of 12 holes in each mirror). The whole structure is very compact and we can estimate the total device footprint to be  $10 \mu\text{m}$  (length of the cavity plus the mirrors)  $\times 0.5 \mu\text{m}$  (waveguide width) =  $5 \mu\text{m}^2$ . For all calculations we have assumed a refractive index of  $n = 3.479$  for Silicon. Design of cavity structures were performed by means of a guided-mode expansion (GME) method, which consists of expanding the magnetic field on the basis of guided modes of an effective homogeneous waveguide and calculating out-of-plane diffraction losses by perturbation theory. [21]

Calculations of transmission spectra and spatial distributions of the electromagnetic field in samples containing cavities within the 500nm waveguide were performed by means of a 3D FDTD method, which consists of solving the Maxwell's equations in space and time without mathematical approximations [22]. The leapfrogging in time followed by implementation of staggered spatial grids leads to an accurate evaluation of the relevant derivatives via finite differences. Absorption of the field components approaching the boundaries of the spatial grids is guaranteed by implementation of the CPML absorbing boundary conditions [23]. A band pass Gaussian pulse with a half-width  $t_w=12.8$  fs and a time delay  $t_0 = 3t_w$  is employed at  $t = 0$  as the initial condition. The numerical simulation of the propagation of this pulse reproduces the conditions of the full-scale study, i.e. a single run of the FDTD program results in time-domain data containing information about the propagation of the electromagnetic field at wavelengths between 1350 and 1630 nm. Transmission spectra are next obtained from these time-domain data using a high-resolution Fourier transform. This range allows that the proposed structure has sufficient capability to be used in optical communication systems due to its desired frequency range. The GME and FDTD methods were also used to optimize the quality factor Q. A number of calculations were performed to evaluate the effect of the number, position and radii of the holes comprising the Bragg reflectors.

### III. SIMULATIONS

The simulated linear transmission spectra and spatial distribution of the electromagnetic field for the structure presented in Fig. 1 are shown in Fig. 2 and Fig. 3, as obtained by using a 2D Finite Difference Time-Domain (FDTD) solver. In particular, this structure is made of a 6 holes mirror, together with 3 holes to taper both the mirror and the cavity, which has 425 nm long spacer section (taken from edge-to-edge of the side holes). The spacing between adjacent holes and the hole radii in the taper region are 300, 315, 325, 65, 80, 85 nm, respectively. The fundamental transverse-electric (TE) guided mode of the PhW waveguide is used as an input propagating pulse to study the device transmittance. We first estimated the propagation waveguide mode in the wire waveguide (3D mode solver) and we obtain an effective index of  $neff=2.915$ . We then used such  $neff$  for the 2D FDTD simulation of the transmission experiment.

A local change in the refractive index of the silicon material around the cavity region is used to simulate the effects of free carrier injection induced by laser pumping at frequencies above the silicon gap. The field intensity for the components is reported in Fig. 3 for off- and in-resonance case, respectively. Out of resonance, at the wavelength of 1550 nm, the light traveling into the guide penetrates the first holes composing the mirror and it is completely reflected backwards. For the resonance case light passes through the mirror and the field is localized in the cavity region. Also the field intensities at resonance are enhanced by as compared to the off-resonance case, as it can be seen from the figure.

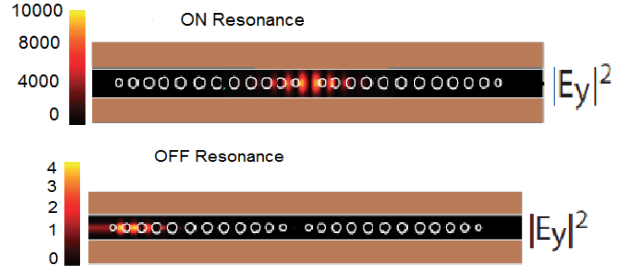


Figure 3. The calculated field intensities at resonance ON and OFF resonance are shown, respectively

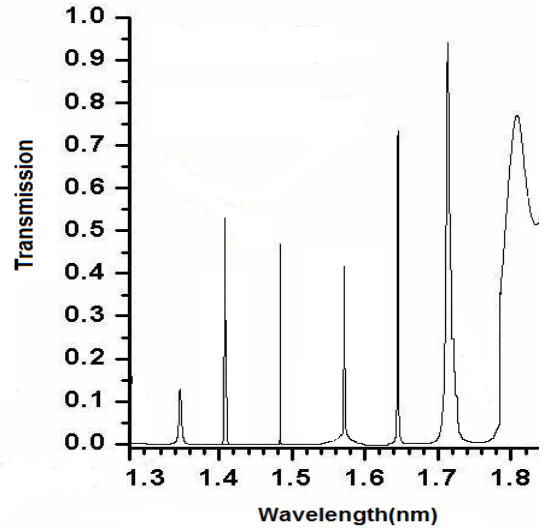


Figure 4. Transmission spectrum for the sample with 425 nm cavity length. The spectrum shows a resonance for the wavelength 1483.547nm with a Q of approximately 160000

The mode volume is very small and close to the diffraction limit, implying strong reduction of power density required for all-optical switching. A 3D FDTD simulation of the cavity mode profile, with excitation by an internal dipole source, gives an effective mode volume :

$$V_{\text{eff}} = \int \epsilon(r) |\mathbf{E}(r)|^2 \frac{dV}{\max\{\epsilon(r)|\mathbf{E}(r)|^2\}} = 0.1\mu\text{m}^3 \sim 1.24 \left(\frac{\lambda}{n}\right)^3$$

### IV. EXPERIMENTAL RESULTS

we show the linear transmittance of a PhC/PhW sample with  $N=4$  periodic holes, a 425 nm cavity spacer length and  $N_{\text{taper}}=4$  number of holes for tapers within the cavity section with  $N_{\text{out}}=3$  is the number of hole outside the cavity. The interference fringes do not prevent the observation of a strong resonance for the wavelength 1483.547 nm with a quality factor  $Q \sim 160000$ .

The inset shows a higher resolution spectrum of the resonance fitted with a Lorentzian line-shape, that was used to determine the Q-factor. The results have successfully been compared with 3D FDTD simulations, which show the photonic stop-band of the mirrors (not fully accessible to our tuning range) as well as the high-Q cavity mode. All-optical switching was achieved by pumping the sample from the top surface to generate free-carriers optically, thereby reducing the refractive index of the silicon backbone and yielding a blue shift of the cavity resonance. In Fig.5 we show the switching behavior of the nanocavity driven by the pump beam, with the probe beam set on resonance with the cavity mode. The temporal evolution of the transmitted probe signal (b), together with the pump beam (a), indicates a clear correspondence between the pulse and the signal - although more complicated phenomena appear after the pulse power decreases. Indeed the rise time of the probe differential transmission follows the pump pulse behavior, while the temporal decay is slower. The recombination dynamics of the free carriers are faster than our temporal resolution - and limited by the pulse duration. However a different phenomenon with a slower time-scale does also play a role in tuning the cavity mode. Most likely, the sample is also heated by the laser pulses and this heating slightly changes the refractive index, yielding a red-shift of the resonance. The energy required for all-optical switching is estimated as follows. The laser beam focused onto the nanocavity has an average power of 7 nW and a pulse energy  $E = 625$  fJ. It is focused on to a spot of about 10 micrometres diameter, which corresponds to an intensity of  $0.3 \text{ kW/cm}^2$ . The calculated carrier concentration is  $0.9 \cdot 10^{18} \text{ cm}^{-3}$  and the Si refractive index variation is  $n = 0.07\%$ . However, only refraction of the beam excites free carriers in the Si photonic wire: if the excited area is estimated to be  $10 \mu\text{m} \times 0.5 \mu\text{m}$ , the deposited energy in the wire is about 37 fJ. Thus, the switching energy is more than two orders of magnitude smaller than demonstrated in previous work on PhC channel waveguides [24].

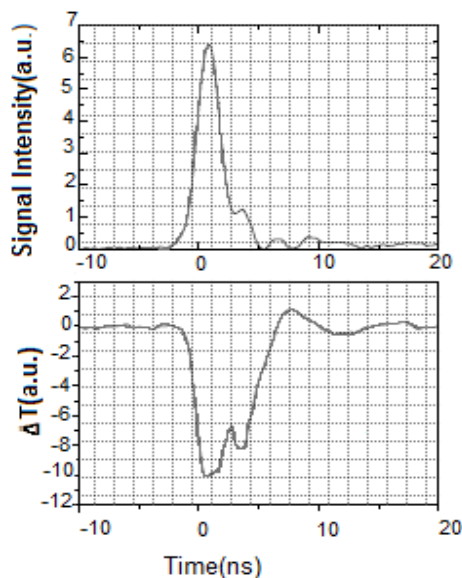


Figure 5. Time evolution of the 532 nm pump pulse employed to inject free carriers into the sample. Change in transmission through the sample at the resonance cavity wavelength 1483.547 nm.

## V. CONCLUSIONS

All-optical switching at very low power levels has been demonstrated in photonic-crystal/photonic-wire nano cavities on silicon-on-insulator with large quality factors and high transmission in the telecom range. The required energy delivered to the silicon wire to obtain full switching with on off behavior is as low as 37 fJ.

## REFERENCES

- [1] J. Poon, L. Zhu, G. DeRose, and A. Yariv, "Transmission and group delay of microring coupled-resonator optical waveguides," *Opt. Lett.* 31, 456 (2006)
- [2] A. Melloni and M. Martinelli, "Synthesis of Direct-Coupled-Resonators Bandpass Filters for WDM Systems," *J. Lightwave Technol.* 20, 296 (2002)
- [3] Bradley Schmidt, Qianfan Xu, Jagat Shakya, Sasikanth Manipatruni, and Michal Lipson, "Compact electrooptic modulator on silicon-on-insulator substrates using cavities with ultra-small modal volumes," *Opt. Express* 15, 3140 (2007), [www.opticsinfobase.org/abstract.cfm?URI=oe-15-6-3140](http://www.opticsinfobase.org/abstract.cfm?URI=oe-15-6-3140)
- [4] I. M'arki, M. Salt, H. Herzig, R. Stanley, L. El Melhaoui, P. Lyan, and J. Fedeli, "Optically tunable microcavity in a planar photonic crystal silicon waveguide buried in oxide," *Opt. Lett.* 31, 513–515
- [5] H. Chong and R. De La Rue, "Tuning of photonic crystal waveguide microcavity by thermo-optic effect," *IEEE Photonics Technol. Lett.* 16(6), 1528–1530 (2004).
- [6] Q. Xu, B. Schmidt, S. Pradhan, and M. Lipson, "Micrometre-scale silicon electro-optic modulator." *Nature* 435, 325–327 (2005).
- [7] B. Schmidt, Q. Xu, J. Shakya, S. Manipatruni, and M. Lipson, "Compact electro-optic modulator on silicon-on-insulator substrates using cavities with ultra-small modal volumes," *Opt. Express* 15, 3140–3148 (2007).
- [8] Q. Xu, S. Manipatruni, B. Schmidt, J. Shakya, and M. Lipson, "12.5 Gbit/s carrier-injection-based silicon microring silicon modulators," *Opt. Express* 15(2), 430–436 (2007).
- [9] S. Manipatruni, Q. Xu, and M. Lipson, "PINIP based high-speed high-extinction ratio micron-size silicon electrooptic modulator," *Opt. Express* 15(20), 13035–13042 (2007).
- [10] K. Preston, S. Manipatruni, A. Gondarenko, C. Poitras, and M. Lipson, "Deposited silicon high-speed integrated electro-optic modulator," *Opt. Express* 17(7), 5118–5124 (2009).
- [11] A. Liu, L. Liao, D. Rubin, H. Nguyen, B. Ciftcioglu, Y. Chetrit, N. Izhaky, and M. Paniccia, "High-speed optical modulation based on carrier depletion in a silicon waveguide," *Opt. Express* 15(2), 660–668 (2007) V. Almeida, C. Barrios, R. Panepucci, and M. Lipson, "All-optical control of light on a silicon chip," *Nature* 431, 1081–1084 (2004).
- [12] T. Tanabe, M. Notomi, S. Mitsugi, A. Shinya, and E. Kuramochi, "All-optical switches on a silicon chip realized using photonic crystal nanocavities," *Appl. Phys. Lett.* 87, 151112 (2005).
- [13] T. Tanabe, K. Nishiguchi, A. Shinya, E. Kuramochi, H. Inokawa, M. Notomi, K. Yamada, T. Tsuchizawa, T. Watanabe, H. Fukuda, et al., "Fast all-optical switching using ion-implanted silicon photonic crystal nanocavities," *Appl. Phys. Lett.* 90, 031115 (2007)
- [14] M. Soljacic and J. Joannopoulos, "Enhancement of nonlinear effects using photonic crystals." *Nat. Mater.* 3(4), 211–219 (2004).
- [15] T. Tanabe, H. Taniyama, and M. Notomi, "Carrier Diffusion and Recombination in Photonic Crystal Nanocavity Optical Switches," *J. Lightwave Technol.*, 26(11), 1396–1403 (2008).

- [16] P. Velha, E. Picard, T. Charvolin, E. Hadji, J. Rodier, P. Lalanne, and D. Peyrade, "Ultra-High Q/V Fabry-Perot microcavity on SILICON-ON-INSULATOR substrate," *Opt. Express* 15, 16090–16096 (2007).
- [17] A.R. Md Zain, M. Gnan, H. Chong, M. Sorel, and R. De La Rue, "Tapered Photonic Crystal Microcavities Embedded in Photonic Wire Waveguides with large Resonance Quality-Factor and High Transmission," *IEEE Photonics Technol. Lett.* 20(1), 6–8 (2008).
- [19] A.R. Md Zain, N. Johnson, M. Sorel, and R. De La Rue, "Ultra high quality factor one dimensional photonic crystal/photonic wire microcavities in silicon-on-insulator (SILICON-ON-INSULATOR)," *Opt. Express* 16(16), 12084–12089 (2008).. P. Lalanne and J. Hugonin, "Bloch-wave engineering for high-Q, small-V microcavities," *IEEE J. Quantum Electron.* 39(11), 1430–1438 (2003).
- [21] L. C. Andreani and D. Gerace, "Photonic-crystal slabs with a triangular lattice of triangular holes investigated using a guided-mode expansion method," *Phys. Rev. B (Condensed Matter and Materials Physics)* 73, 235114 (2006).
- [22] A. Taflove and S. Hagness, *Computational electrodynamics: the finite-difference time-domain*
- [23] C. Sauvan, G. Lecamp, P. Lalanne, and J. Hugonin, "Modal-reflectivity enhancement by geometry tuning in Photonic Crystal microcavities," *Opt. Express* 13(1), 245–255 (2005).
- [24] T. Tanabe, K. Nishiguchi, A. Shinya, E. Kuramochi, H. Inokawa, M. Notomi, K. Yamada, T. Tsuchizawa, T. Watanabe, H. Fukuda, H. Shinojima, and S. Itabashi, 'Fast all-optical switching using ionimplanted silicon photonic crystalnanocavities,' *Appl. Phys. Lett.* 90,031115 (2007).